Japanese Journal of Applied Physics

The Japan Society of Applied Physics

REGULAR PAPER • OPEN ACCESS

Characterization of non-uniform InGaN alloys: spatial localization of carriers and optical properties

OPEN ACCESS

Japanese Journal of Applied Physics **58**, SCCC03 (2019) **REGULAR PAPER**

https://doi.org/10.7567/1347-4065/ab06ba

Characterization of non-uniform InGaN alloys: spatial localization of carriers and optical properties

A. Di Vito[1], A. Pecchia[2], A. Di Carlo[1], and M. Auf der Maur[1*]

[1]*Department of Electronics Engineering, University of Rome Tor Vergata, Via del Politecnico 1, 00133 Rome, Italy*
[2]*CNR-ISMN, Via Salaria Km 29.300, 00017 Monterotondo (Rome), Italy*

*E-mail: auf.der.maur@ing.uniroma2.it

Received December 23, 2018; revised January 12, 2019; accepted January 18, 2019; published online April 16, 2019

Statistical indium fluctuations in InGaN alloys have been demonstrated to induce spatial localization of carriers. This phenomenon has a strong influence on the behavior of InGaN based light emitting diodes and it is further exacerbated by the presence of compositional non-uniformities. In the present work, we theoretically characterize non-uniform InGaN alloys, taking into account the impact of indium clustering on the electronic and optical properties of the material. The assumption of a non-uniform indium distribution within the bulk structure results in a reduction of the band gap energy and a broadening of the absorption edge with respect to the uniform random alloy configuration, in agreement with the experimental results found in literature. Moreover, we find that it is crucial to consider the presence of compositional non-uniformity in order to derive a theoretical description that is consistent with the outcomes of the experimental studies, especially when the indium content exceeds 10%. Such an effect suggests that a growing indium concentration yields an increment in the amount of indium clustering. Finally, we use the Getis–Ord statistics in order to derive the characteristic localization length of the carriers. This is an original application of this method, usually employed in geospatial analysis. © 2019 The Japan Society of Applied Physics

1. Introduction

Indium Gallium Nitride (InGaN) alloys have gained increasing attention in the last decades due to their successful application in optoelectronic devices. InGaN is the most advanced material for the realization of green-blue-violet light emitting diodes (LEDs)[1,2] and blue-violet laser diodes.[3] In particular, the efficiency of InGaN/GaN quantum well LEDs, emitting in the wavelength range below 460 nm, was demonstrated to exceed 70%.[4]

Despite the commercial success of these devices, there are several issues, such as the efficiency droop and the green gap problem, which are still debated in the literature[5–8] and are partly related to the structural and electronic properties of the material. In particular, the role of compositional non-uniformity in the spatial localization of carriers and its impact on the performance of InGaN devices has not been extensively discussed. As a matter of fact, previous simulation studies have been performed assuming a uniform indium distribution within the alloy.[5,6,9–11] However, such an assumption does not allow to study structures with increasing degree of disorder, inducing translational symmetry breaking and pronounced carrier localization. On the other hand, the presence of indium clusters has been proposed to have a strong influence on the LED behavior, leading to potential fluctuations that limit the non-radiative recombination of carriers.[12] In particular, Ref. 13 have studied the influence of localizing valence states associated with In-N zigzag atomic chains on the emission properties of indium containing nitride alloys, using experimental techniques. Moreover, a theoretical description of the spatial localization of carriers induced by the intrinsic formation of In-N zigzag chains and quantum dots in InGaN alloys is reported in previous studies.[14,15] However, the mentioned arrangements do not resemble the atomic configuration obtained when only slight to medium deviations from the uniform random alloy structure are taken into account.

Motivated by the lack of a statistical characterization of the phenomena related to compositional non-uniformity in InGaN, in this work we analyze the properties of the bulk alloy where the distribution of indium atoms is not uniform. The amount of deviation from a uniform random alloy configuration is defined in Sect. 2, where we describe the method employed for the generation of the samples and the computational approach used to perform the simulations. In Sect. 3.1, we discuss the impact of indium fluctuations on the spatial localization of carriers. We compare the results obtained from empirical tight binding (ETB) and density functional theory (DFT) calculations for a small uniform random alloy periodic supercell. The influence of compositional non-uniformity on the carrier localization is considered in Sect. 3.2, where we use the Getis–Ord statistics[16] to detect the presence of indium clusters within the structure and derive the degree of localization and the characteristic localization length of the carriers. This is the first application of the Getis–Ord statistics in the field of condensed matter physics. Finally, in Sect. 3.3, we study the effect of a non-uniform indium distribution on the band gap energy and the optical absorption edge of $In_xGa_{1-x}N$, for several values of the mean indium content x. We find that the non-uniformity induces a broadening of the absorption edge, as also pointed out in recent experimental results.[17] Moreover, our analysis suggests that the non-uniformity is more pronounced when the mean indium content increases.

2. Theoretical approach

In order to analyze the effect of statistical indium fluctuations on the carriers' spatial localization of bulk $In_xGa_{1-x}N$, we first simulated several random alloy supercells, composed of 288 atoms, with a uniform indium distribution. The indium content was set to $x = 0.02$, 0.1 and 0.2. The electronic structure was calculated with two different approaches: the ETB,[18,19] using the TiberCAD software,[20] and the

DFT,[21,22] using the QuantumEspresso package.[23] DFT simulations were performed with a non relativistic norm conserving Goedecker–Hartwigsen–Hutter–Teter type pseudopotential for indium and gallium atoms and a scalar relativistic norm conserving Von Barth-Car type pseudopotential for nitrogen atoms. The Perdew–Zunger exchange-correlation energy[24] was used in both cases. The plane wave energy cutoff was set to 100 Ry and the Brillouin Zone (BZ) was sampled at the Γ point only. In all the considered settings, the structure was relaxed according to the valence force field (VFF) theory.[25] The results of the simulations are discussed in Sect. 3.1.

With the aim of investigating the impact of compositional non-uniformity on the alloy properties, we then considered a $10 \times 10 \times 10\,\mathrm{nm}^3$ $In_xGa_{1-x}N$ supercell at several degrees of non-uniformity.

The uniform samples were generated by randomly substituting gallium atoms with indium atoms and assuming a spatially uniform substitution probability equal to the mean indium concentration. Differently, for the non-uniform alloy, we first uniformly distributed a certain percentage of indium atoms, denoted in the following as the percentage of uniformity in order to identify the different structures. The remaining indium atoms were then distributed with a spatially varying probability as follows. We first picked a gallium atom randomly. Then we counted the indium atoms around this gallium up to the second nearest cation site, and we calculated the substitution probability as the ratio of this number and the available cation sites, therefore leading to a spatial correlation. This was repeated until all necessary indium atoms were distributed. Note that, in order to fix the mean indium content, the total number of indium atoms was kept constant. The degree of clustering can be controlled by the percentage of uniformly distributed indium atoms: the lower the percentage, the more clustering can be expected.

To obtain the electronic and optical properties, we used the atomistic ETB approach, since the supercell size is out of the reach of DFT. The atomistic structures were first relaxed using a VFF method. Then, we computed the first eight electron and twelve hole states in four points of the reduced BZ, from which we calculated the momentum matrix elements, optical spectra and density of states.

The outcomes of such simulations are discussed in Sects. 3.2 and 3.3 for the spatial localization of carriers and the optical properties, respectively. In Sect. 3.2, we set the mean indium content to $x = 0.2$ and we considered the following percentage of uniformity: 100% (random alloy), 80%, 60% and 40%. Differently, in Sect. 3.3 we analyze the cases where $x = 0.05$, 0.10, 0.15 and 0.20 for 80% and 60% uniform structures. To obtain statistically significant results, we simulated 50 structures for the uniform random alloy configuration, as well as for the slightly clustered alloy (80% uniformity). For the other cases, we used 100 random samples since the statistical variations are more pronounced for the strongly clustered structures.

3. Results and discussion

In the present section, we report and analyze the outcomes of our simulations. In Sect. 3.1, we discuss the role of indium fluctuations in the spatial localization of carriers. In particular, we show that the ground state hole wave function is localized within indium rich regions. Such an effect is exacerbated by the presence of indium clusters, as we demonstrate in Sect. 3.2, where we use the Getis–Ord statistics in order to quantify the degree of compositional non-uniformity and derive the characteristic localization length of the carriers. The Getis–Ord method is standardly used in geospatial analysis. Nevertheless, we show that the mentioned statistics is a powerful tool also for the description of non-uniform atomic structures. Finally, we discuss the impact of compositional non-uniformity on the electronic and optical properties of the bulk material, in terms of energy gap and optical absorption. We show that the presence of indium clusters induces a reduction of the band gap energy with respect to the uniform alloy and a broadening of the absorption edge, in agreement with the experimental results found in literature.

3.1. Spatial localization of carriers in uniform InGaN alloys

In this section, we show the projected density of states (PDOS) on some significant nitrogen atoms and the respective isosurface of the ground state hole wave function for one sample structure with indium content $x = 0.2$. All the analyzed quantities refer to a 288-atom periodic supercell. The results are obtained using both the ETB and the DFT approaches, where DFT calculations do not include the effect of spin–orbit coupling. We discuss the role of statistical fluctuations of the indium content on the carriers' localization and compare our outcomes with the relevant related literature.

ETB and DFT calculations of the PDOS are compared in Fig. 1. The associated 3D-structures are shown in Fig. 2, where the isosurface of the ground state hole wave function is depicted in yellow. For both theoretical approaches, it is clear that the first hole state is localized on nitrogen atoms placed within indium rich regions. This effect is particularly evident if we compare the PDOS on nitrogen atom 188 (close to indium) with the PDOS on nitrogen atom 44, in Fig. 1. We can observe that the PDOS associated to the first states of the valence band is much higher on the nitrogen atom that is located close to indium atoms. These results are confirmed by the isosurfaces of the ground state hole wave function represented in Fig. 2. The enhanced amplitude of this state on nitrogen sites close to indium atoms is clearly evident, for both ETB and DFT calculations, as demonstrated in previous studies.[5,6,10,26–28] Moreover, the outcomes of the two theoretical approaches are in very good qualitative agreement, except for the value of the band gap energy, deduced by the PDOS in Fig. 1. As a matter of fact, it is well known that DFT calculations in the framework of local density approximation yields a substantial underestimation of the band gap energy.

3.2. The role of compositional non-uniformity in the spatial localization of carriers

In this section, we consider a $10 \times 10 \times 10\,\mathrm{nm}^3$ $In_{0.2}Ga_{0.8}N$ supercell, at several degrees of non-uniformity. The simulations are performed using the ETB approach. The generation of the samples with different amounts of uniformity is discussed in Sect. 2.

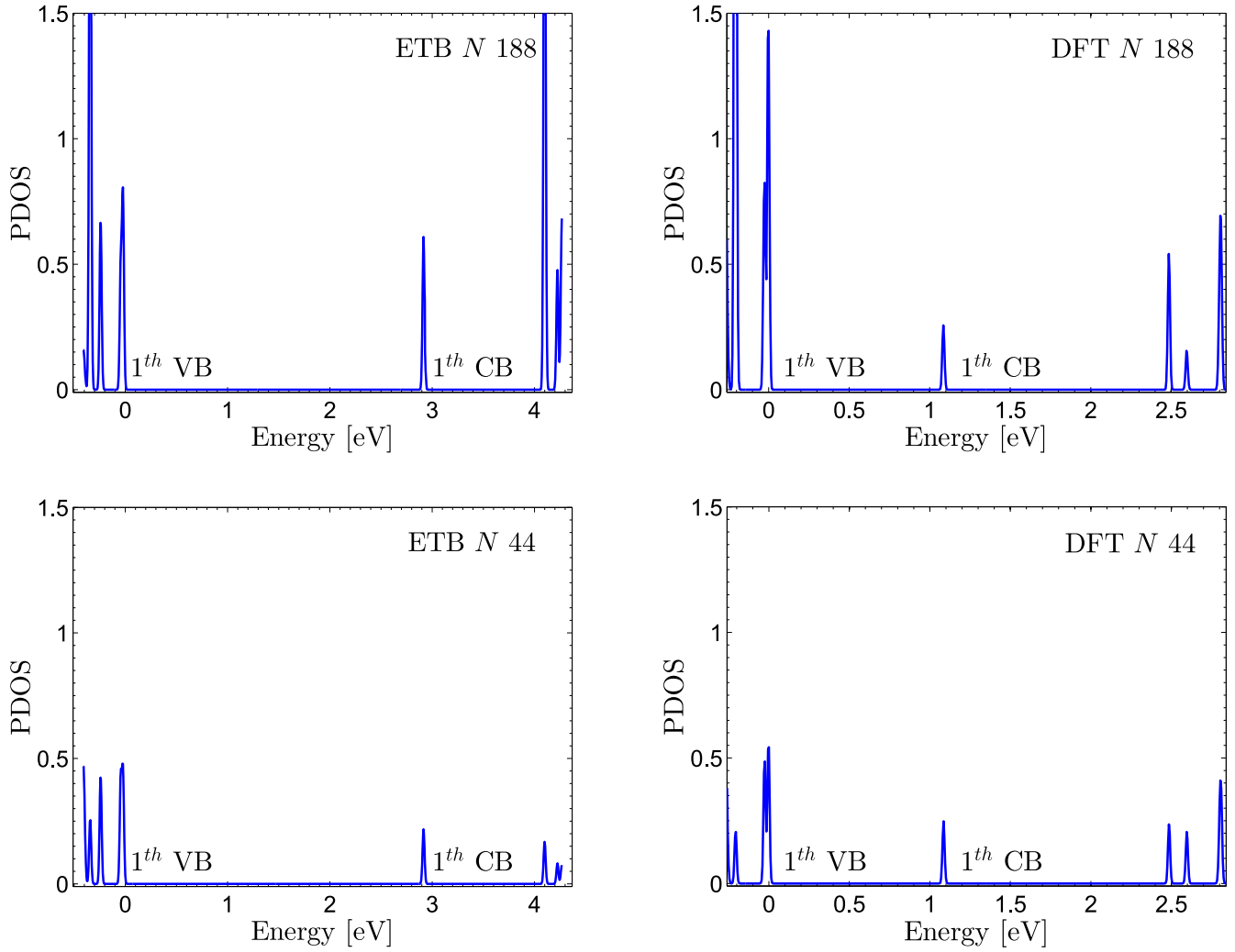

Fig. 1. (Color online) PDOS on some nitrogen atoms of interest in an $In_{0.2}Ga_{0.8}N$ 288-atom supercell (the structure is shown in the previous figure). ETB calculations on the left and DFT calculations on the right.

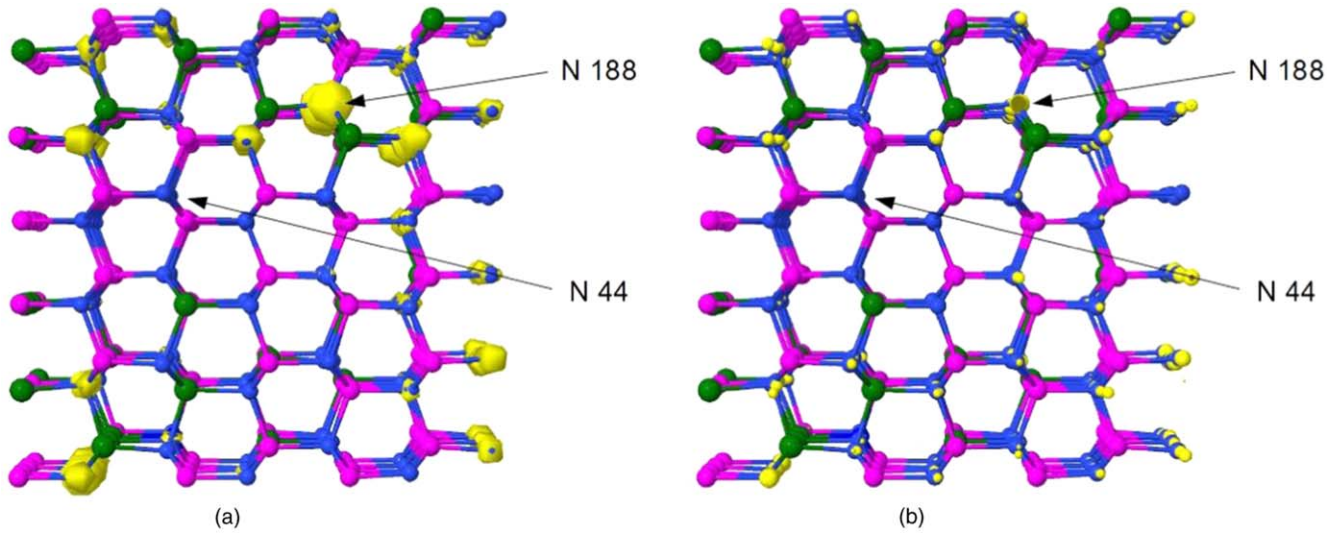

Fig. 2. (Color online) Ground state hole wave function (yellow) for a bulk $In_{0.2}Ga_{0.8}N$ random alloy derived with (a) an ETB approach and (b) a DFT approach. Indium, gallium and nitrogen atoms are depicted in green, magenta and blue, respectively. The supercell is composed of 288 atoms. A relatively high isovalue is used for the plot, in order to highlight the spatial localization of the wave function.

In order to characterize the degree of clustering in the atomistic structures and in the wave functions, we analyze the carrier spatial localization using the Getis–Ord global statistic. This statistics tool is an interesting method to quantify the presence of spatial clusterization of high and low values. In its standardized form, it is defined as[16)]

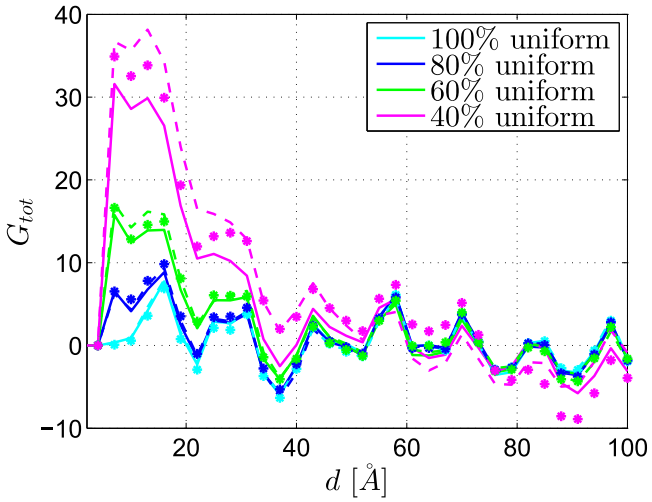

Fig. 3. (Color online) Getis–Ord global statistic for the structural analysis of a bulk $In_{0.2}Ga_{0.8}N$ alloy at several percentage of uniformly distributed indium atoms, resulting in several degrees of clustering. The three different line styles represent the results for three different samples at each degree of clustering.

$$G_{\mathrm{tot}}(d) = \frac{\sum_i \sum_j w_{ij}(d)(x_j - \bar{x})(x_i - \bar{x})}{s\sqrt{\frac{n^2 \sum_i \sum_j w_{ij}(d) - \left(\sum_i \sum_j w_{ij}(d)\right)^2}{n^2 - 1}}}, \quad (1)$$

where $\bar{x} = \sum_j x_j / n$ and $s^2 = \sum_i (x_i - \bar{x})^2 / n$. The total number of atoms is n, and the function $w_{ij}(d)$ is defined as

$$w_{ij} = \begin{cases} 1 & \text{if } d_{ij} \leqslant d \\ 0 & \text{if } d_{ij} > d \end{cases} \quad (2)$$

with d_{ij} the distance between the i-th and j-th atoms. Positive significant values of G_{tot} indicate the presence of clusters of high values, while clustering of low values are represented by negative relevant values of G_{tot}. The value of d where G_{tot} takes a maximum can be interpreted as the characteristic length of clustering.

In order to analyze the atomistic structure using the G_{tot} statistic, x_i is set to one if the i-th atom is an indium, and to zero otherwise. Figure 3 shows the resulting $G_{\mathrm{tot}}(d)$. We can observe that for the 100% uniform structure no significant clustering of indium atoms can be deduced, while increasing non-uniformity leads to increasing clustering with growing values of G_{tot}.

For the analysis of the localization of the electronic states, we set x_i to the PDOS on atom i at specific energies associated to the states of interest, in particular the electron and hole ground states. In this case, the Getis–Ord global statistic can be interpreted as a measure of the carriers' spatial localization, since high values of G_{tot} indicate spatial clustering of the probability density. Figures 4(a) and 4(b) show $G_{\mathrm{tot}}(d)$ for the first electron and the first hole state, respectively. As expected, for the 100% uniform structures G_{tot} is almost zero for all d values and for both the electron and hole ground state. However, related to the increasing clustering of indium atoms shown in Fig. 3, we observe growing clustering of high probability density values, and thus localization of the carriers. This is confirmed by the isosurfaces of the ground state electron and hole wave functions, depicted in Fig. 5. The localization behavior of electrons and holes is slightly different, as expected. The hole ground state exhibits substantial localization in the 80% uniform structures, while the electron ground state starts to localize only between 80% and 60% of uniformity. From the figures we can also see a decrease of the characteristic localization length, which must be expected, since it should transition from infinite, for a delocalized state, to roughly the characteristic size of the indium clusters. Note that the characteristic length for clustering is of the order of the largest supercell sizes typically used for DFT based calculations. This shows that results obtained from such studies can not be expected to provide insight into weak spatial localization in random or slightly non-uniform alloys.

3.3. Electronic and optical properties of non-uniform InGaN alloys: the influence of indium fluctuations

Here, we discuss the influence of compositional non-uniformity on the band gap energy and the optical absorption

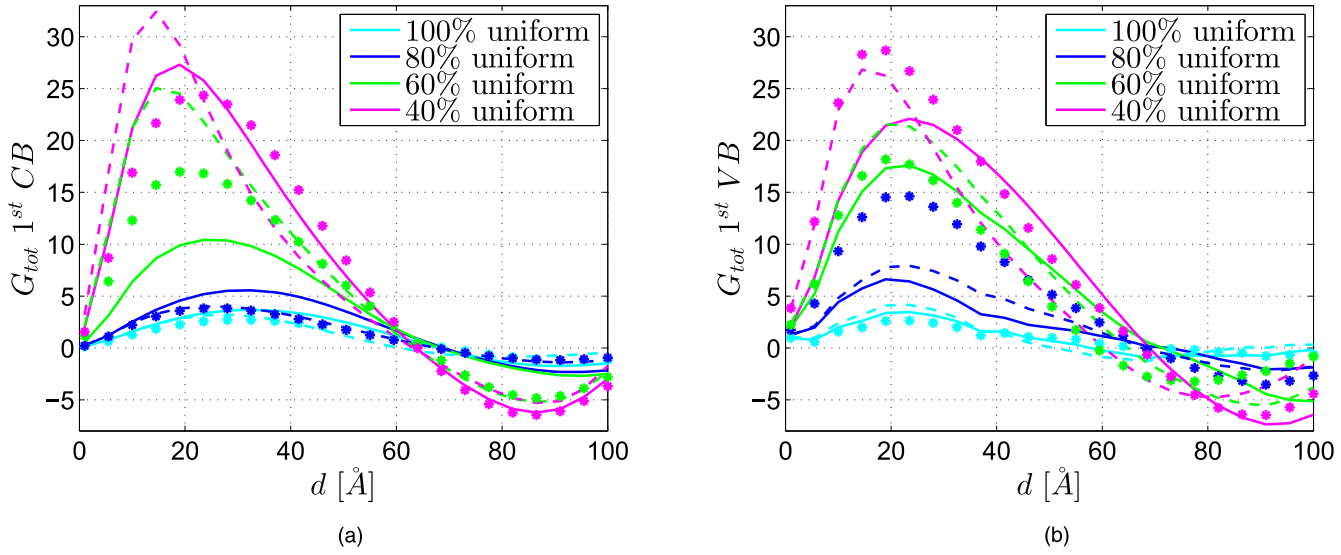

Fig. 4. (Color online) Getis–Ord global statistic for (a) the first electron state and (b) the first hole state of a bulk $In_{0.2}Ga_{0.8}N$ alloy at several percentage of uniformly distributed indium atoms, resulting in several degrees of clustering. The three different line styles represent the results for three different samples at each degree of clustering.

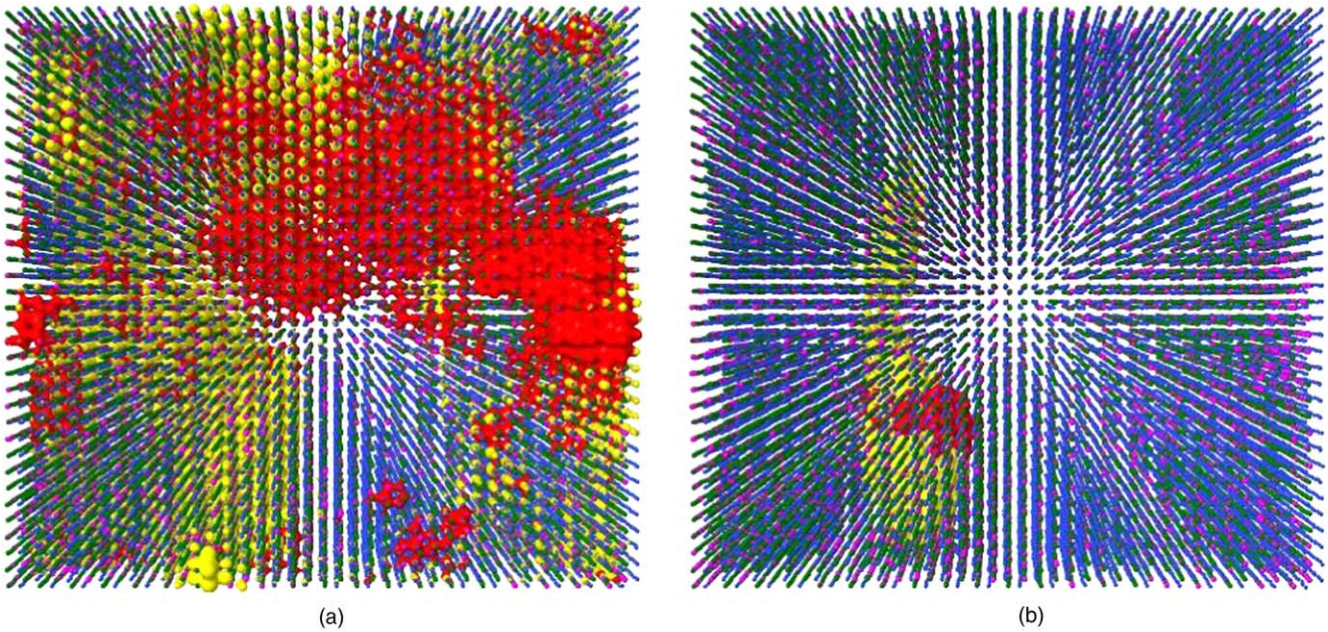

Fig. 5. (Color online) Ground state electron (red) and hole (yellow) wave functions for a bulk $In_{0.2}Ga_{0.8}N$ alloy with (a) 100% (uniform alloy) and (b) 40% (maximum clustering degree) of uniformly distributed indium atoms. The isosurfaces containing (a) 10% and (b) 50% of the total ground state density are shown. Indium, gallium and nitrogen atoms are depicted in magenta, green and blue, respectively. The supercell side length is 10 nm.

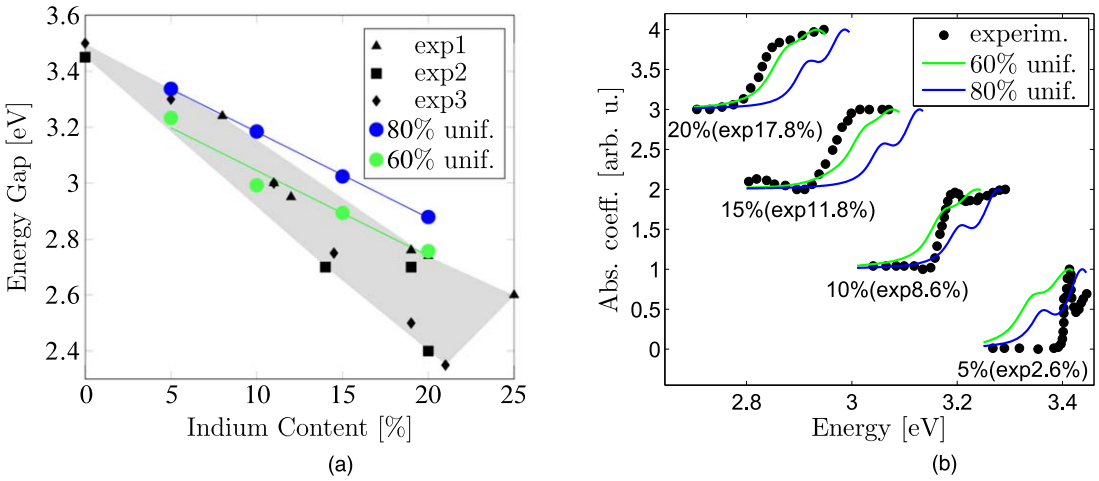

Fig. 6. (Color online) (a) Energy gap of $In_xGa_{1-x}N$ as a function of indium content x, expressed in percentage. Calculations are shown for the 80% (blue circles) and 60% (green circles) uniform alloy. Measured optical energy gaps of $In_xGa_{1-x}N$ are depicted by black triangles (exp1[29]), black squares (exp2[30]) and black diamonds (exp3[31]). (b) Absorption coefficient (sample average) of bulk $In_xGa_{1-x}N$ for several values of indium content x, expressed in percentage. Calculations are shown for the 80% (blue line) and 60% (green line) uniform alloy. Measured optical absorption edge spectra (black circles) from Ref. 17 are also shown. The indium content of the experimental samples (specified in brackets) is slightly different from the value used to perform the simulations. Each set of spectra is vertically shifted for clarity.

edge of bulk $In_xGa_{1-x}N$. Regarding the definition of the degree of uniformity and the details about the computational approach, we refer to Sect. 2.

In Fig. 6(a), we report the band gap energy as a function of indium content derived for the 80% and 60% uniform alloy, depicted by blue and green circles, respectively. We can see that the results obtained for the 60% uniform structure match very well the experimental band gap values (black markers) and the composition dependence of the band gap energy deduced by the measurements (represented by the shaded area). Differently, the theoretical band gap energy of the 80% uniform samples agrees with the experimental outcomes only in the range of low indium content. This effect can be qualitatively explained if we assume that the non-uniformity increases for increasing indium concentration. Thus, based on the results shown in Fig. 6(a), we can reasonably state that the compositional fluctuations are more pronounced when the content of indium increases.

Concerning the optical properties of the non-uniform $In_xGa_{1-x}N$ alloy, we analyze the behavior of the optical absorption edge as a function of the composition and the amount of uniformity, shown in Fig. 6(b). Here, we consider the mean absorption coefficient derived from the statistical ensembles for each indium content and clustering degree, i.e. $\bar{\alpha} = 1/n\sum_i \alpha_i$ where α_i is the absorption coefficient for each random structure and n is the ensemble size. Thus, we study the macroscopic behavior of the sample rather than the effects of a particular atomic arrangement, assuming that

the macroscopically measured absorption spectra can be interpreted as a spatial average over a sample region.[5)]

In Fig. 6(b), we observe an increasing broadening of the optical absorption edge with increasing indium content and clustering degree. This trend is in good agreement with the experimental results (black circles) reported by Ref. 17 on thick InGaN layers. In particular, as the percentage of indium increases, a washing out of a double peak structure at the absorption edge is observed in the measured spectra. Such an effect is well described by the calculations performed on the 60% uniform structures (green line), especially when the indium content exceeds 10%. On the other hand, the results derived for the 80% uniform samples (blue line) agrees with experiment only for low indium concentrations. This behavior suggests that growing indium content leads to increased non-uniformity, as discussed in the previous paragraph. Thus, the optical absorption edge broadening observed by Butté et al. is likely due to increasing non-uniformity in the indium distribution.

4. Conclusions

In this work, we characterized $In_xGa_{1-x}N$ alloys where the presence of compositional non-uniformities is explicitly taken into account.

First of all, we showed that statistical fluctuations of the indium content induce the carriers to spatially localize within indium rich regions, in agreement with results found in literature. Such an effect is further exacerbated by the presence of indium clusters, as we demonstrated analyzing structures with several degrees of non-uniformity in the indium distribution. In particular, we used the Getis–Ord statistics in order to quantitatively describe the amount of clustering and derive the characteristic localization length of the carriers. This is the first application of the mentioned statistics in the field of condensed matter physics.

Furthermore, we considered the influence of compositional fluctuations on the optical properties of the alloy. We found that an increasing non-uniformity in the indium distribution causes the band gap energy to decrease with respect to the uniform random alloy configuration and induces a broadening of the optical absorption edge. This behavior agrees very well with the experimental results found in literature.

Finally, our study showed that it is important to account for the presence of indium clusters in order to derive a theoretical description that properly matches the experimental outcomes, especially when the mean indium content exceeds 10%. This suggests that growing indium concentration leads to increased compositional non-uniformity.

Acknowledgments

This work has been supported by Horizon 2020 project ChipScope, under grant agreement number 737089.

1) S. Nakamura, M. Senoh, and T. Mukai, Jpn. J. Appl. Phys. **32**, L8 (1993).
2) S. Nakamura, T. Mukai, and M. Senoh, Appl. Phys. Lett. **64**, 1687 (1994).
3) S. Nakamura, M. Senoh, S. I. Nagahama, N. Iwasa, T. Yamada, T. Matsushita, H. Kiyoku, and Y. Sugimoto, Jpn. J. Appl. Phys. **35**, L74 (1996).
4) Y. Narukawa, M. Ichikawa, D. Sanga, M. Sano, and T. Mukai, J. Phys. D: Appl. Phys. **43**, 354002 (2010).
5) M. Auf der Maur, A. Pecchia, G. Penazzi, W. Rodrigues, and A. Di Carlo, Phys. Rev. Lett. **116**, 027401 (2016).
6) C. M. Jones, C. H. Teng, Q. Yan, P. C. Ku, and E. Kioupakis, Appl. Phys. Lett. **111**, 113501 (2017).
7) J. Piprek, Phys. Status Solidi A **207**, 2217 (2010).
8) E. Taylor, P. R. Edwards, and R. W. Martin, Phys. Status Solidi A **209**, 461 (2012).
9) D. Oriato and A. B. Walker, Physica B **314**, 59 (2002).
10) T. J. Yang, R. Shivaraman, J. S. Speck, and Y. R. Wu, J. Appl. Phys. **116**, 113104 (2014).
11) D. Watson-Parris, M. Godfrey, P. Dawson, R. Oliver, M. Galtrey, M. Kappers, and C. Humphreys, Phys. Rev. B **83**, 115321 (2011).
12) S. Chichibu, T. Azuhata, T. Sota, and S. Nakamura, Appl. Phys. Lett. **70**, 2822 (1997).
13) S. Chichibu et al., Nat. Mater. **5**, 810 (2006).
14) P. R. C. Kent and A. Zunger, Appl. Phys. Lett. **79**, 1977 (2001).
15) L.-W. Wang, Phys. Rev. B **63**, 245107 (2001).
16) A. Getis and J. K. Ord, Geographical Anal. **24**, 189 (1992).
17) R. Butté et al., Appl. Phys. Lett. **112**, 032106 (2018).
18) J. M. Jancu, R. Scholz, F. Beltram, and F. Bassani, Phys. Rev. B **57**, 6493 (1998).
19) J. M. Jancu, F. Bassani, F. D. Sala, and R. Scholz, Appl. Phys. Lett. **81**, 4838 (2002).
20) M. Auf der Maur et al., Opt. Quantum Electron **40**, 1077 (2008).
21) P. Hohenberg and W. Kohn, Phys. Rev. **136**, B864 (1964).
22) W. Kohn and L. J. Sham, Phys. Rev. **140**, A1133 (1965).
23) P. Giannozzi et al., J. Phys.: Condens. Matter **21**, 395502 (2009).
24) J. P. Perdew and A. Zunger, Phys. Rev. B **23**, 5048 (1981).
25) D. Camacho and Y. Niquet, Physica E **42**, 1361 (2010).
26) X. Wu, E. J. Walter, A. M. Rappe, R. Car, and A. Selloni, Phys. Rev. B **80**, 115201 (2009).
27) B. Lee and L. W. Wang, J. Appl. Phys. **100**, 093717 (2006).
28) L. Bellaiche, T. Mattila, L. W. Wang, S. H. Wei, and A. Zunger, Appl. Phys. Lett. **74**, 1842 (1999).
29) J. Wu, W. Walukiewicz, K. Yu, J. Ager III, E. Haller, H. Lu, and W. J. Schaff, Appl. Phys. Lett. **80**, 4741 (2002).
30) G. Franssen et al., J. Appl. Phys. **103**, 033514 (2008).
31) M. Moret, B. Gil, S. Ruffenach, O. Briot, C. Giesen, M. Heuken, S. Rushworth, T. Leese, and M. Succi, J. Cryst. Growth **311**, 2795 (2009).